TECHNICAL REPORT

No. 2/85

A S R - THERMODYNAMICS

RESULTS OF A NUMERICAL SIMULATION
AND SURFACE TEMPERATURE MEASUREMENTS

by

G. Lemperle
DFVLR Stuttgart

IEA- OPERATING AGENT
DEUTSCHE FORSCHUNGS- UND VERSUCHSANSTALT
FÜR LUFT- UND RAUMFAHRT e.V.

ASR - THERMODYNAMICS

Results of a Numerical Simulation and Surface Temperature Measurements

Internal Report IB 444-006/85

G. Lemperle

D F V L R - Stuttgart

CONTENTS

1. NUMERICAL SIMULATION

The computer code HOTREC was used to calculate the thermodynamic behavior of the ASR-Receiver. The code is briefly described in Ref.1. Based on the partial differential equations describing the energy balance for the tube wall, the heat carrier sodium and the ceramic backwall the simulation code has the following characteristics

1. Heat conduction in tube wall in radial and in the direction of the circumference.

2. Heat transfer to sodium using heat transfer coefficient.

3. Radiation exchange between tube surface, ceramic backwall and environment calculated separately in the visible and infrared wavelength. Application of the 'enclosure method' (Ref.2).

4. Losses by convection (using correlations of Ref.3).

5. Spatial angle dependent heat flux distribution (HELIOS) serves as input parameter.

To compare the code with other calculations concerning ASR-Thermodynamics (Ref.3 or Ref.4) steady state conditions has been calculated. The ASR is described in detail elsewhere (Ref.3 and Ref.5). At design point the following results were obtained:

Incident Power	2760 KW
Absorbed Power	2486 KW

Fig.1 and Fig.2 represents the corresponding flux density distribution.

Losses

Reflection	116 KW
Convection	80 KW
Emission	78 KW

Sodium

Inlet Temperature	270 C
Outlet Temperature	530 C
Flow Rate	7.3 kg/sec

The losses by reflection were determined using an effective Emissivity of $\varepsilon_{eff} = 0.9576$. A structured surface like a tube panel produces an effective emissivity which is larger than that of a flat plate. The exact correlation for a tube panel with no space between the tubes would be the solution of a Fredholm-Integral, which analytically is difficult to get. But there is a range in between the effective emissivity has to be (see Ref.10).

$$\varepsilon(1 + (1-\varepsilon)(1-2/\pi)) < \varepsilon_{eff} < \varepsilon / (1 - (1-\varepsilon)(1-2/\pi))$$

Assuming $\varepsilon = 0.935$ yields $\varepsilon_{eff} \approx 0.957$. This value approximately corresponds to the measurements of R. Carmona (Ref.6). Since the measurement port of the emissivity measurement device is larger than the diameter of one tube, the measured datas are effective emissivities. The losses by emission are based on calculations using an effective emissivity in the infrared wavelenth of $\varepsilon_{eff} = 0.9$.

The optical properties of the Pyromark coating are responsible for the amount of absorption and emission. Its high temperature resistance and excellent optical behavior favours Pyromark for solar application. But there is one disadvantage of Pyromark. Its thermal conductivity is very bad compared to metal. As reported in Ref.7 Pyromark 2500 consists of 100 percent silicone resin. The addition of refractory pigments provides the flat black color. By vitrification the silicone resins are converted to inorganic silica producing a thin refractory coating. For silica one finds thermal conductivities reaching from $\lambda = 0.6 - 1.8$ W/m/K. Even if the thickness of the coating is very small compared to the tube wall there may be the same temperature gradient through Pyromark as through the tube wall. For the ASR the original thickness of the Pyromark layer was measured, and had an average value of 45 Microns (Ref.8). This yields a higher front surface temperature. As a consequence the losses may be increased a bit (for design conditions approximately 15 KW additional losses). But this doesn't affect the temperature distribution in the tube wall significantly.

The results of the numerical simulation with HOTREC for design condition are presented in Fig.3 - Fig.8 . Fig.3 - Fig.7 show the heat flux and the temperature profiles along the tube length. Sodium inlet is on the right side sodium outlet on the left. Fig.8 represents the temperature profile in the tube wall of tube no. 98 at 1.7m above the lower aperture rim. Arcus 0 corresponds to the front side of the tube, arcus π to the back side of the tube facing the ceramic backwall. For steady state at design condition a maximum outer metal temperature of T = 597.°C is reached. The results agree essentially with calculations of other simulation codes (Ref.3, Ref.4).

2. MEASSUREMENT OF SURFACE TEMPERATURE BY USING AN INFRARED IMAGING SYSTEM

As a part of the HERMES-System the infrared camera was applied to measure the front surface temperature distribution during the measurement campaign in autumn 1984. The specifications of the camera are described in Ref.1. The thermodynamic and optical properties of the surface affects strongly the surface temperature. Since the measurement is physcally based on infrared radiation a variation in the emissivity results in measurement errors. If the variation of the emissivity is less than 1.5% this yields an error of ±8 K As there are some more sources of errors (see Ref.1) the sum of them (applying the Gauss-Correlation) yields a total error of ±10 K.

The intention of the temperature measurements was to get datas about typical operating conditions as there are steady state, transient behaviour, start up, shut down and partial load. In the following some results concerning steady state are presented. The datas were measured on December 12th, 1984. Due to heliostat failures (89 of 93 heliostats were in operation), increased shading and blocking, reduced mirror reflectivity (r=0.8) and insolation (I=800 W/m/m) the power to the receiver is about 40% smaller than for design conditions. Fig.9 shows the isothermal lines of the front surface of the tubes at 9:42:00h solar time. At that time we had steady state conditions. The thermodynamic parameters of the ASR taken from the Class Summery Report of the DAS are listed below:

Receiver inlet temperature	262.0 C
Receiver outlet temperature	530.6 C
Sodium Flow	20.9 m**3/h

The surface temperature exceeds 600 ^{0}C on the 5th panel. But one has to keep in mind that this is the surface temperature of the Pyromark coating. As mentioned in chapter 1 there is an increased surface temperature of the Pyromark compared to the metal temperature.

The 3D-presentation of the temperature distribution (Fig.10) gives an impression about the shape of the distribution. Fig.11 - Fig.15 show some vertical temperature profiles of the front surface along the tube length. The top of the receiver tubes corresponds to 0.635m the bottom to 3.365m.

Fig.16 and Fig.17 represents horizontal temperature profiles. Especially Fig.16 points out the panel design of th ASR. Panel 1 is on the very left side and has the lowest temperature which approximately is equal to the sodium inlet temperature since the flux density is very small in the lower left edge of the receiver. Panel 5 is characterized by the highest inlet temperature of about 440. C. Fig.17 is a horizontal cross section of the temperature distribution where the highest surface temperatures occur at 1.86m above the lower aperture rim. There the maximum surface temperature of 626. C was measured on the 5th panel.

Knowing the measured surface temperature distribution the HERMES-Software calculates the losses by infrared emission of the whole receiver and of each panel. Assuming an emissivity in the infrared wavelength range of ε_{eff}=0.9 the losses are:

total emission		102 KW
emission	panel 1	9 KW
	panel 2	9 KW
	panel 3	17 KW
	panel 4	28 KW
	panel 5	39 KW

3. COMPARISON CALCULATION-MEASUREMENT

To compare the measurements shown in chapter 2 with calculations by HOTREC the meteo, heliostat field and thermodynamic datas belonging to this conditions are used. The calculation provides:

Incident power	1766 KW
Losses	
reflection	75 KW
emission	77 KW
convection	77 KW

The thickness of Pyromark layer was assumed to be 45 Microns the thermal conductivity 0.6 W/m/K. The isothermal lines of the front surface temperature for this calculation is shown in Fig.18 and as a 3D-Presentation in Fig.19. The shape has to be compared with Fig.9 and Fig.10. Obviously the shape of the measurement and the calculation are very similar. A more detailed comparison is presented by Fig.20. Measured and calculated temperature profiles of tube 98 are plotted versus the tube length. Its the calculated and measured Pyromark surface temperature which has to be compared to judge the agreement between calculation and measurement. The maximum value of th measurement is higher than the calculated one. There may be two reasons to explain the difference:

1. The thermal conductivity of Pyromark used for the calculation may be smaller than assumed.

2. After the refilling incident (September 1983) and the following repair of the distorted tubes some tubes were repainted with Pyromark by brushing and the thickness of the layer might have been increased.

That means both the thickness of the coating and the correct value of the thermal conductivity are necessary and has to be measured.

Regarding the shape of the measured temperature profile there is a dip just above the half of the tube length. This observation fits very well with the emissivity measurements of R.Carmona and M.Geyer (Ref.9). They detected on the 5th panel an emissivity degradation in the same region where the temperature dip occurs. As written above variation of the emissivity is the main error for infra-

red measurements. But nevertheless there is still a good agreement between calculation and measurement. As a consequence the code HOTREC seems to be a tool to simulate the thermodynamic behavior correctly.

4. HIGH FLUX EXPERIMENT

To achieve flux densities of about 2.5MW/sqm at the SSPS/CRS it is necessary to change the aiming strategy for the ASR. If there is only one aim point at (0.,0.) one gets the flux distribution shown in Fig.21 and Fig.22. Here only Martin-Marietta heliostats are used to concentrate solar radiation on ASR. A maximum flux of 2.48 MW/sqm is reached. This distribution served as input for the simulation code HOTREC to calculate the temperature distribution and efficiency. As a consequence of the high flux the losses will be reduced a bit. The values are listed below:

Incident power	2868 KW
Losses	
reflection	121 KW
emission	77 KW
convection	79 KW

Fig.23 and Fig.24 are showing the temperature profiles of the outer tubes of panel 4. The average metal temperature difference of those two tubes is responsible for the distortion of the panel. For design conditions they were limited to 40 C. Fig.25 represents the expected heat flux and temperature profile along tub 98 where the highest temperature occurs and the focus point is situated. There one has to expect a maximum metal temperature of 685 C and a maximum temperature gradient along the circumference of the tube of 165 C.

5. REFERENCES

(1) Lemperle, G.
Schiel, W.
Efficiency and Temperature Measurements.
Workshop of the IEA/SSPS Deliverable
Reviews, Oct. 15-18., 1984
Proceedings in Preparation.

(2) Hottel, H.C.
Sarrofim, A.F.
Radiative Transfer.
McGraw-Hill 1967.

(3) Agip Nucleare,
Franco Tosi
The Advanced Sodium Receiver.
Topic Reports.
SSPS Technical Report No. 3/83 Vol. 1+2.

(4) De Benedetti, A.
Blanco, M.
Comparison with Simulation.
Workshop of IEA/SSPS Deliverable
Reviews, Oct. 15-18.,1984
Proceedings in Preparation.

(5) Hansen, J.
SSPS-CRS Advanced Sodium Receiver.
Construction Experience Report.
SSPS SR5, Sept. 1984

(6) Carmona, R.
Sanchez, M.
Absorptance Measurement of the Advanced
Sodium Receiver.
SSPS Internal Report, Doc. no. R57-85MSRC
March 14, 1985

(7) Communication
Channels, Inc.
High Temperature Coatings from Space!
Modern Paint+Coating, Oct. 1978

(8) Bedogni, V.
Thickness of Pyromark Coating.
Privat Communication.
March 1985.

(9) Geyer, M.
Absorptivitaetsmessungen am ASR-Receiver.
SSPS Internal Report, 2/85
14.3.1985.

(10) Kast, W.
Die Erhöhung der Wärmeabgabe durch
Strahlung bei mehrfacher Reflexion
zwischen strahlenden Flächen.
VDI-Verlag GmbH, Düsseldorf, March 1965

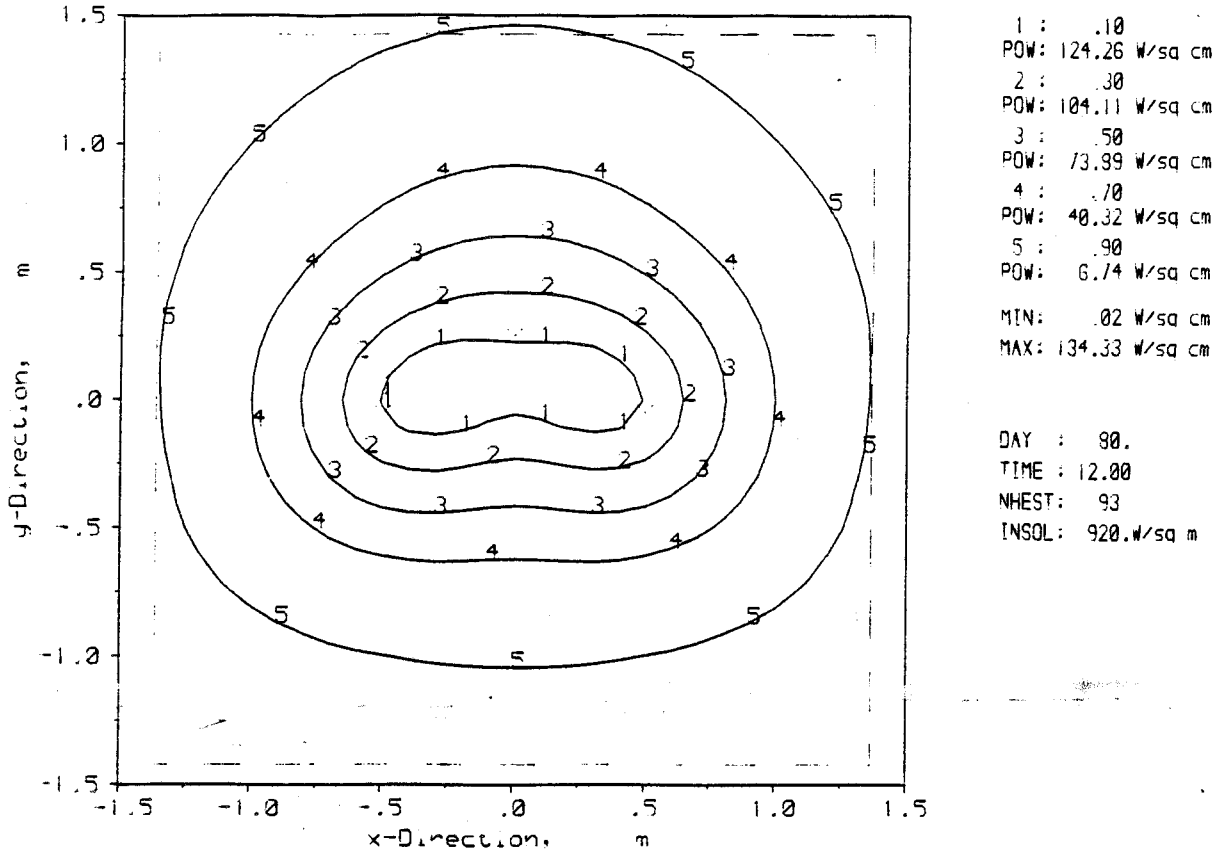

Fig.1: Isolines of flux distribution for design conditions; aim points (.0,.25), (-.50,-.05), (.50,-.05)

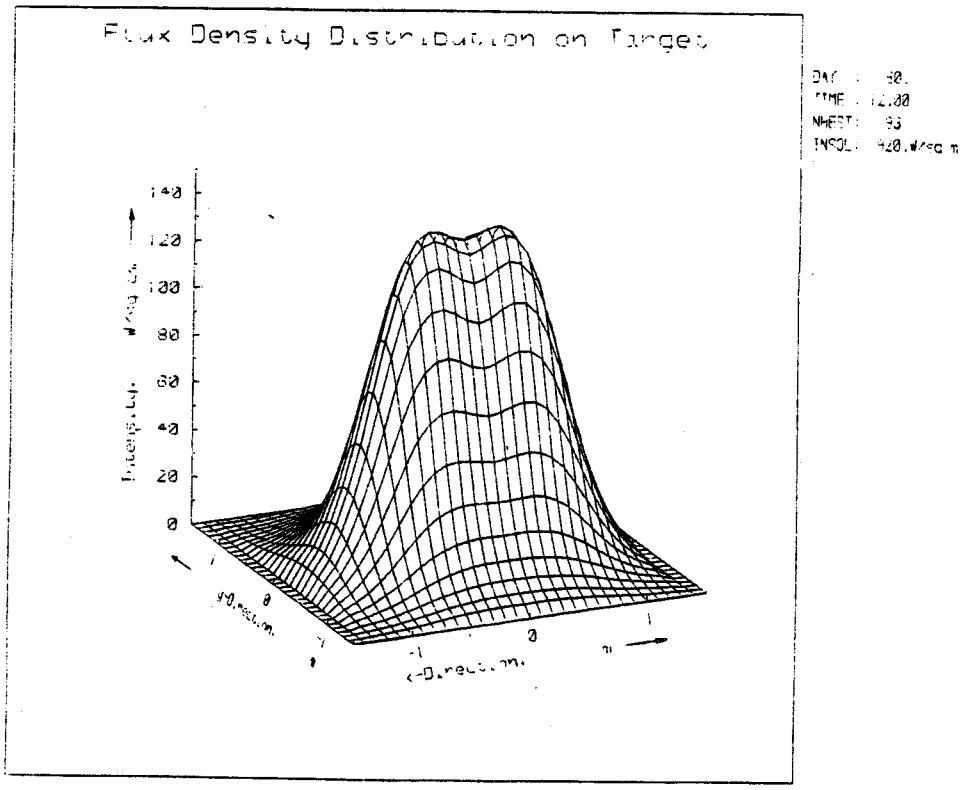

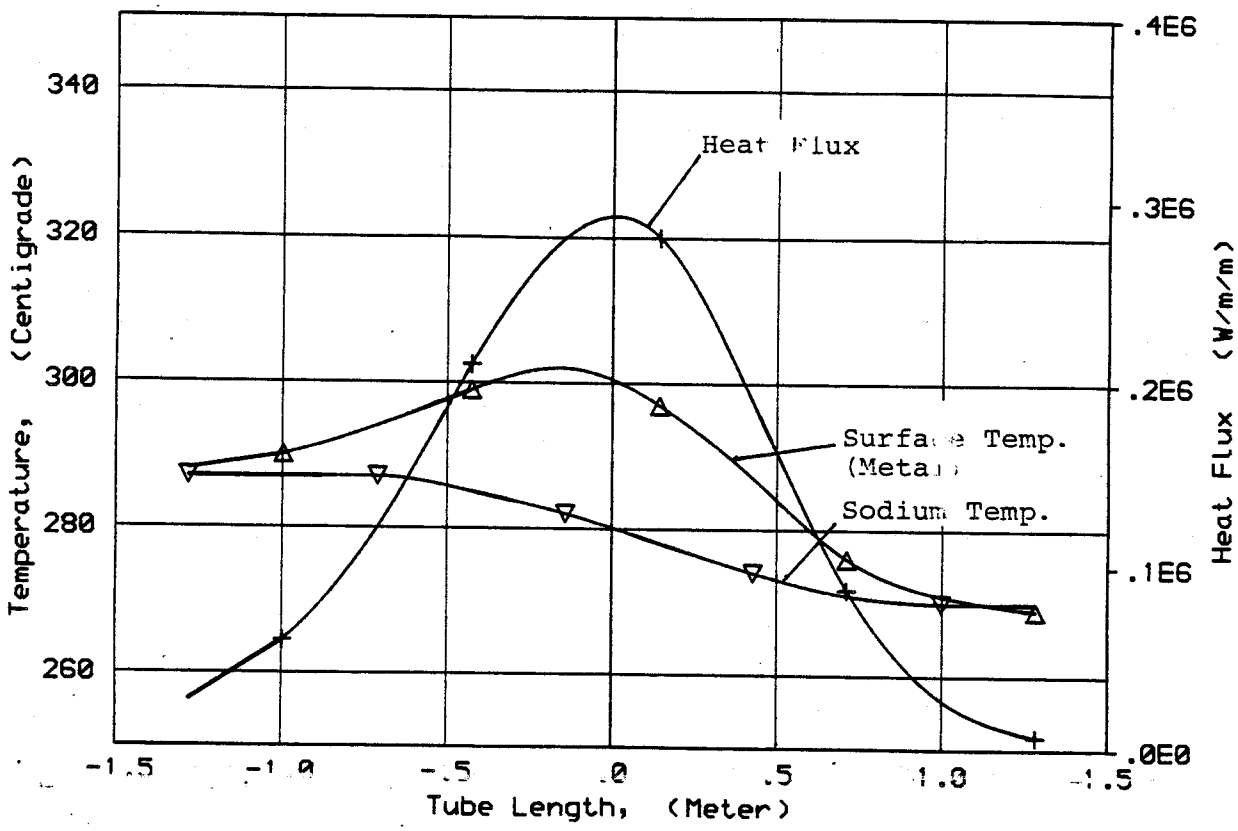

Fig.3: Temperature and Heat Flux vs. Tube Length (Tube 19); Design Conditions; Steady state

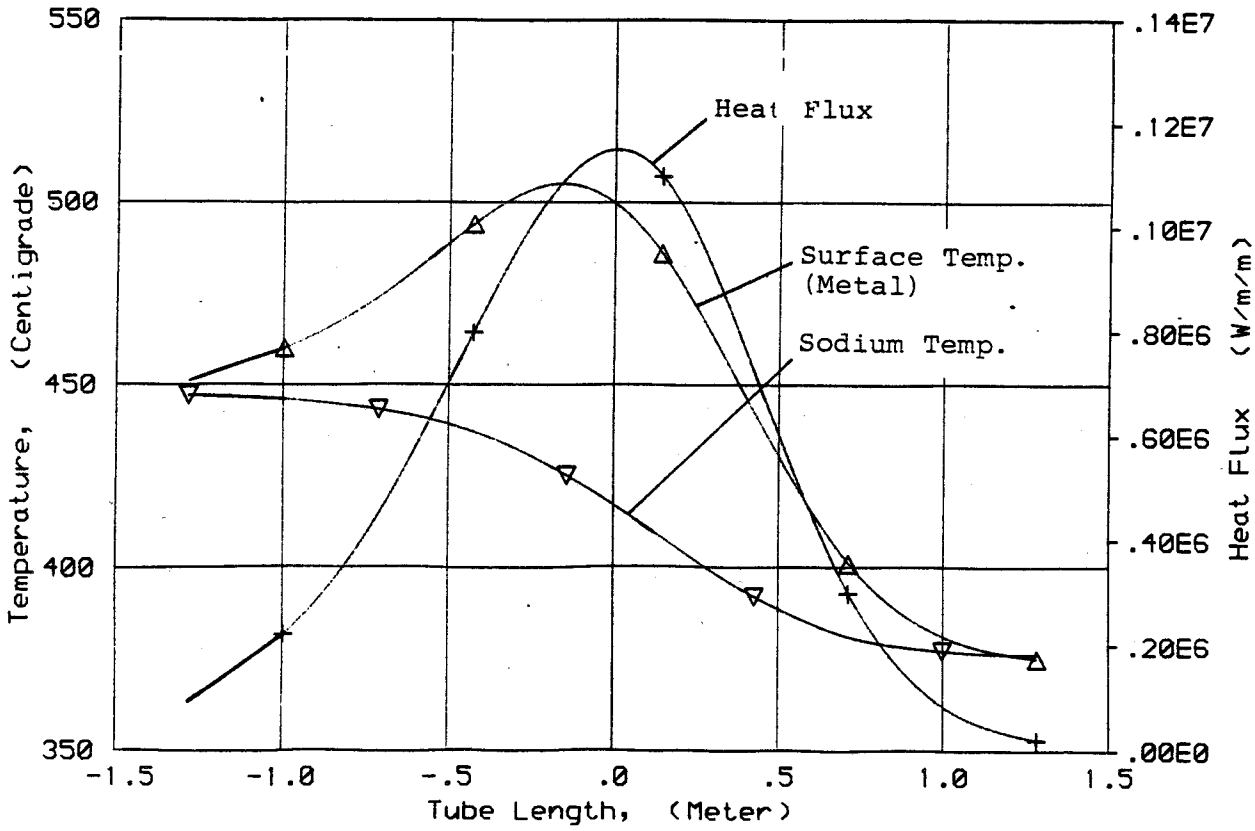

Fig.4: Temperature and heat flux vs. tube length (tube 59); Design conditions; steady state.

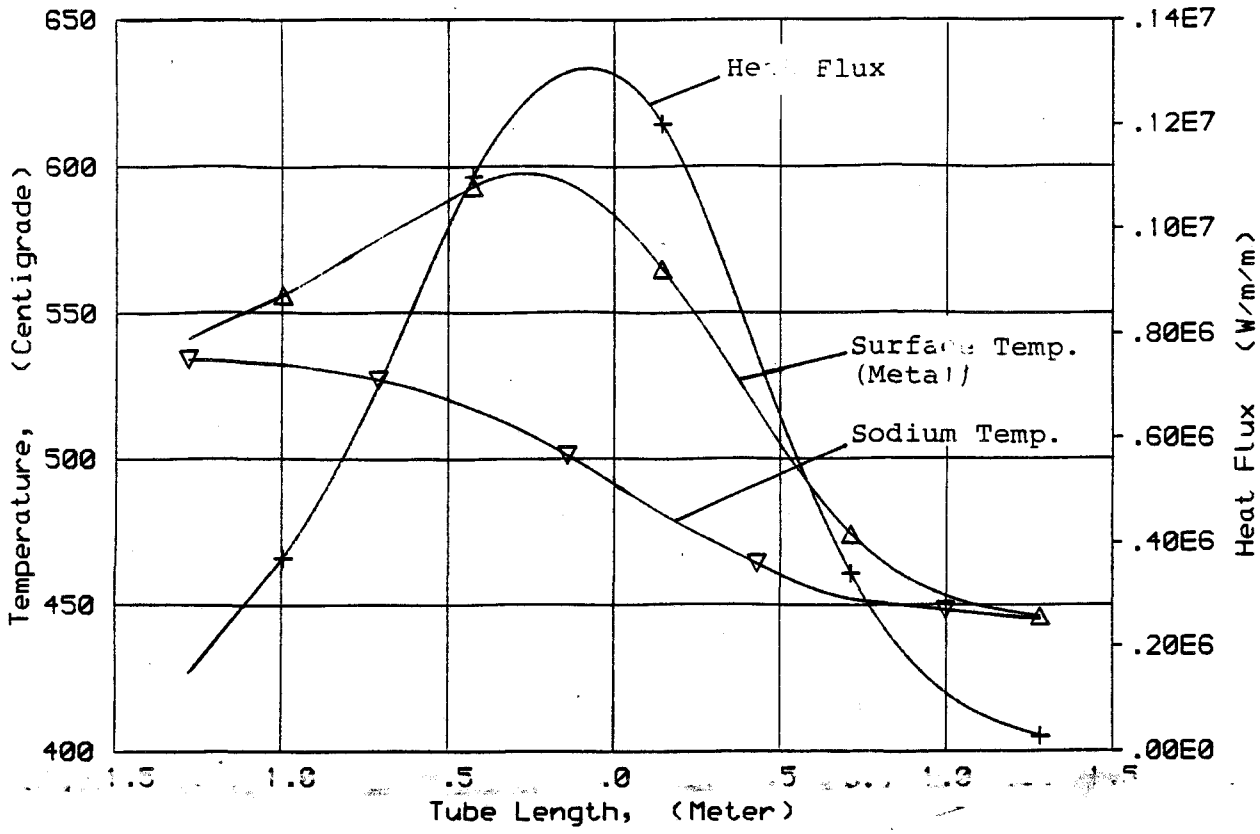

Fig.5: Temperature and heat flux vs. tube length (tube 98); design conditions; steady state

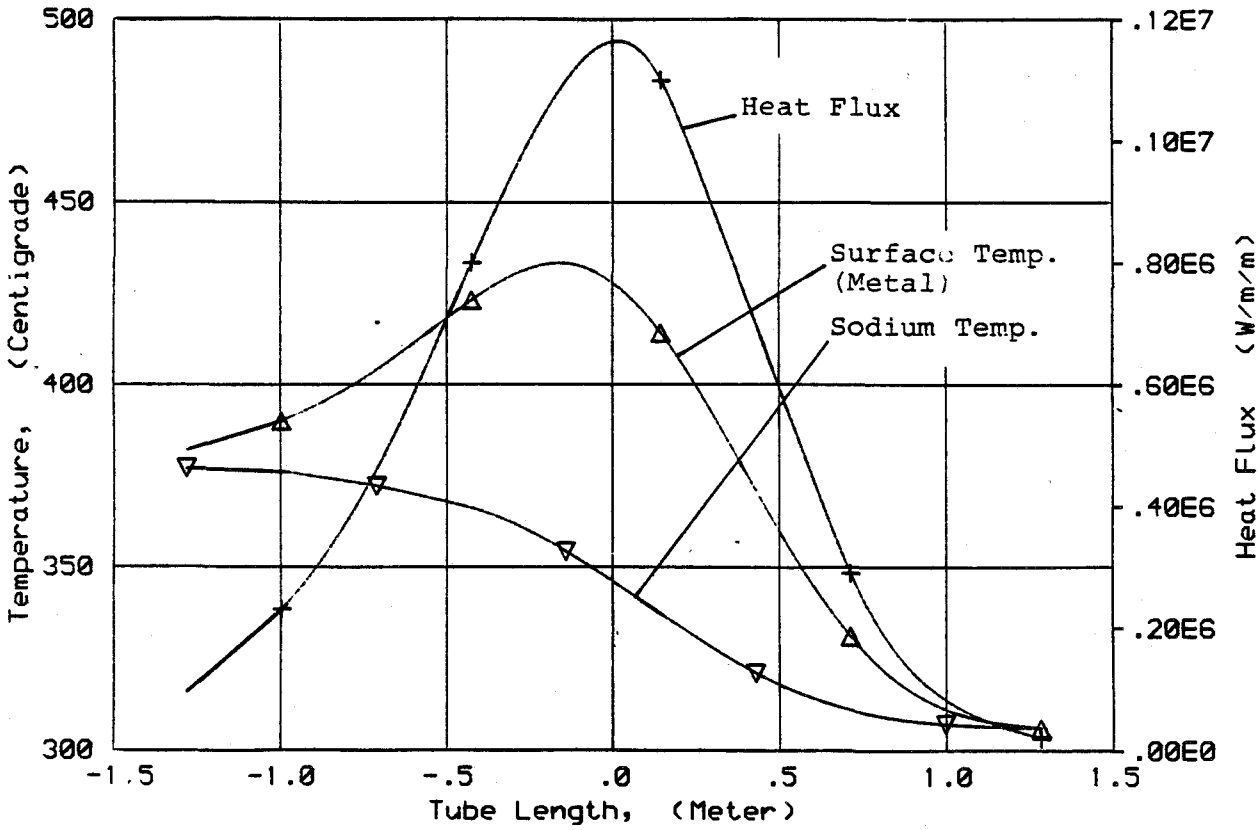

Fig.6: Temperature and heat flux vs. tube length (tube 137); design conditions; steady state.

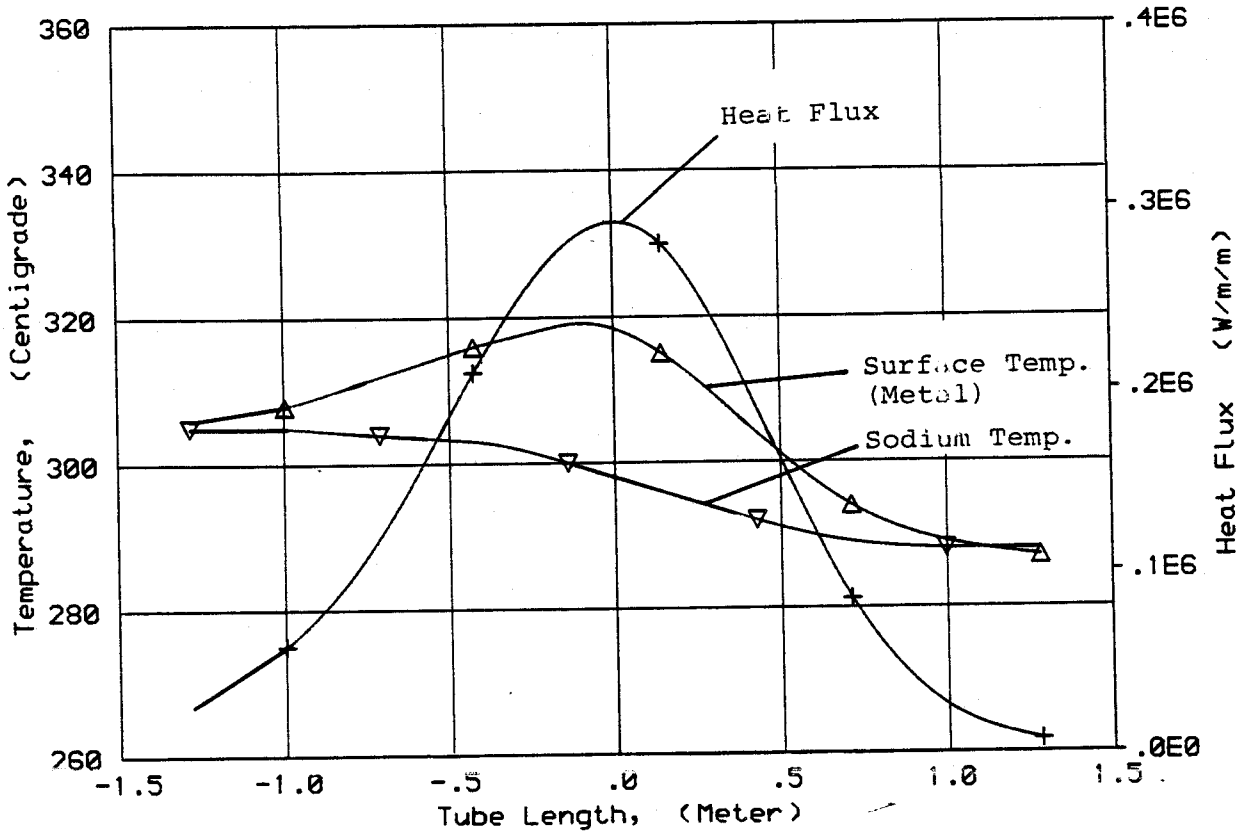

Fig.7: Temperature and heat flux vs. tube length (tube 176); design conditions; steady state.

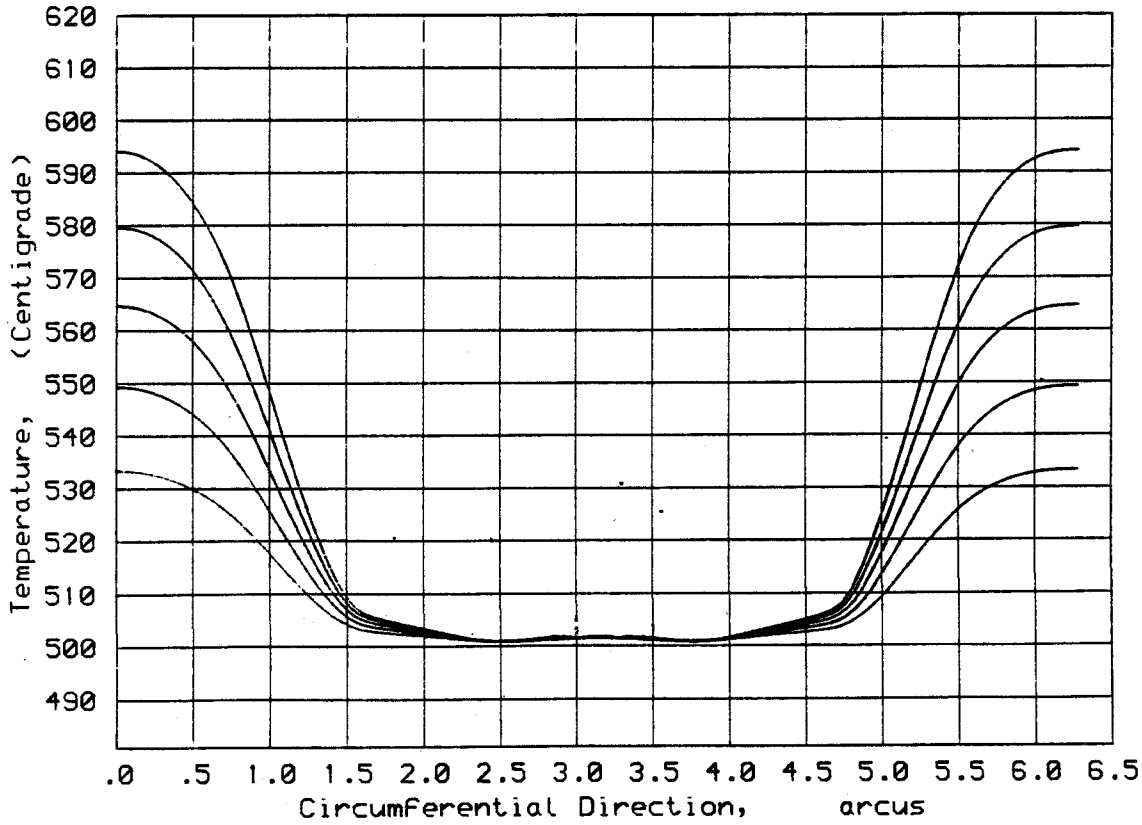

Fig.8: Tube wall temperature vs. circumference (tube 98, at 1.7m height); most upper curve - outer surface, lowest curve - inner surface.

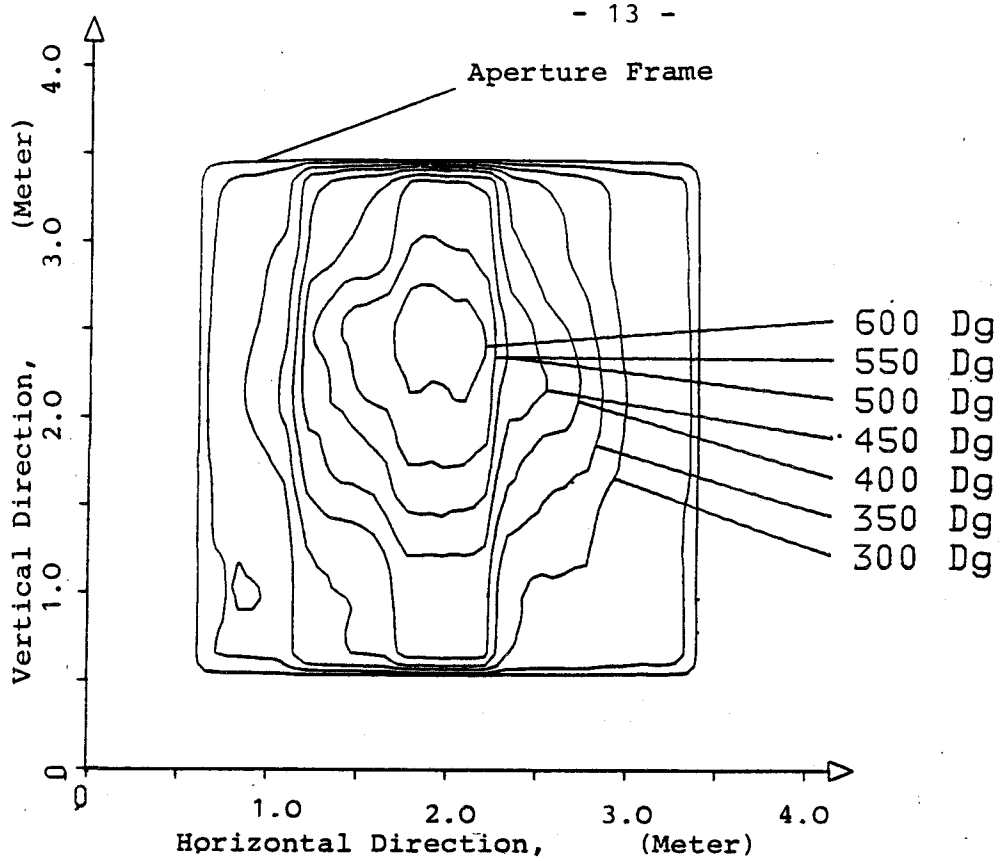

12-Dec-84 10:44:43

Weather

Windvel.	4.90 m/s
Winddir.	79.92 Degs
Humidity	59.26 %
Tempert.	12.00 C-Dg

Radiance

Dir.-1	808.20 W/m2
Dir.-2	788.06 W/m2
Diffuse	51.84 W/m2
Glb.Hrz.	367.08 W/m2
Glb.Gdd.	947.14 W/m2

Circumsolar

Factor	0.00 %

Sun Location

Sol.time	9.69 hrs
Elevat.	21.54 Degs
Azimuth	325.84 Degs
Declin.	-23.11 Degs
Ascens.	259.75 Degs
Longit.	260.58 Degs

Fig.9: Isothermal lines of front surface ASR (Pyromark Coating); measured by Infrared Camera (HERMES).

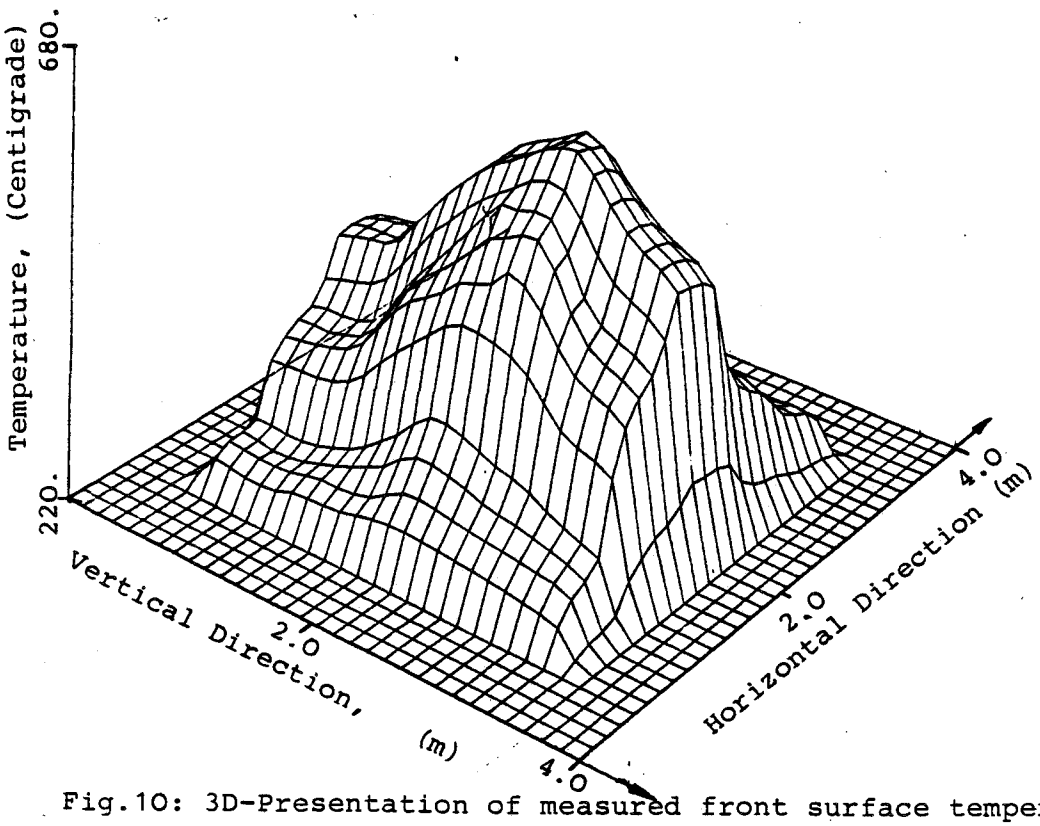

12-Dec-84 10:44:43

Weather

Windvel.	4.90 m/s
Winddir.	79.92 Degs
Humidity	59.26 %
Tempert.	12.00 C-Dg

Radiance

Dir.-1	808.20 W/m2
Dir.-2	788.06 W/m2
Diffuse	51.84 W/m2
Glb.Hrz.	367.08 W/m2
Glb.Gdd.	947.14 W/m2

Circumsolar

Factor	0.00 %

Sun Location

Sol.time	9.69 hrs
Elevat.	21.54 Degs
Azimuth	325.84 Degs
Declin.	-23.11 Degs
Ascens.	259.75 Degs
Longit.	260.58 Degs

Fig.10: 3D-Presentation of measured front surface temperature ASR.

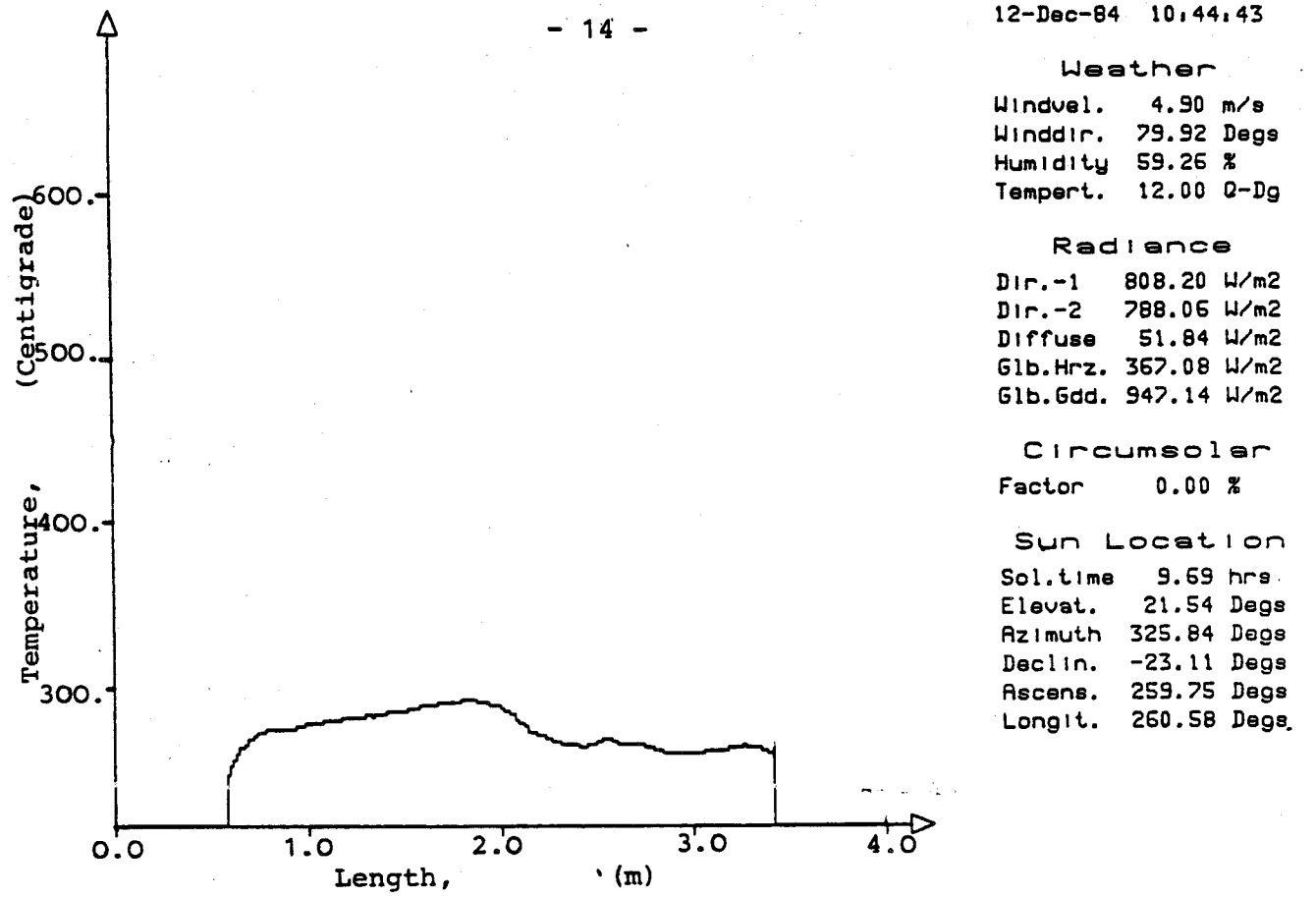

Fig.11: Vertical surface temp. profile (measured); in the region of tube 11 sodium inlet at 3.365m, sodium outlet at .635m.

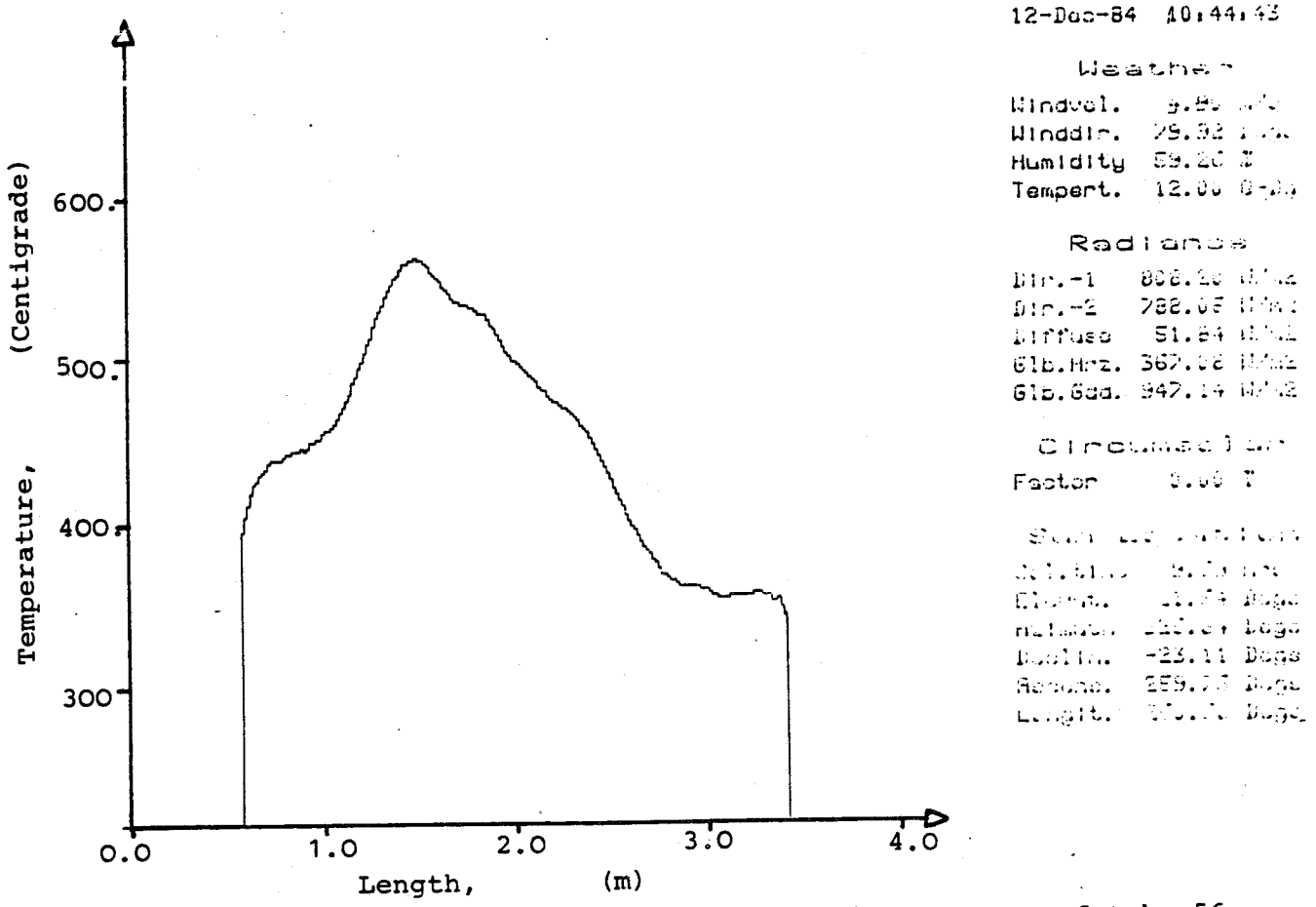

Fig.12: Vertical surface temp. profile(measured);in region of tube 56

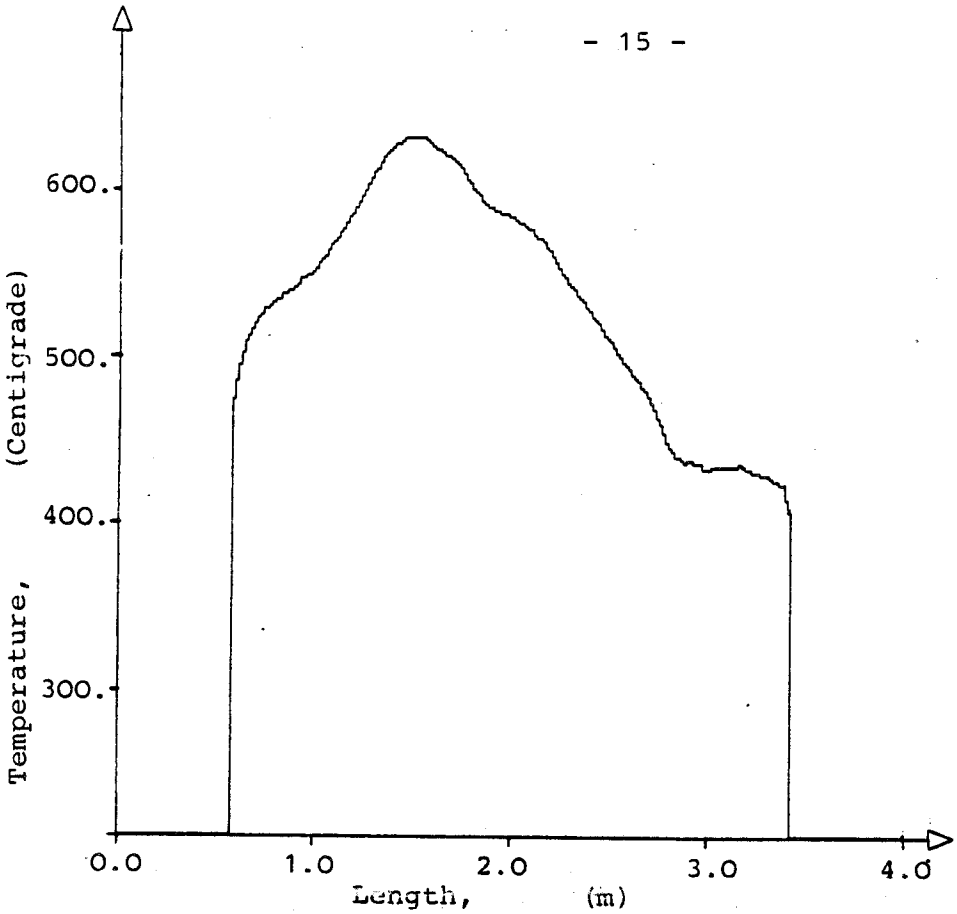

12-Dec-84 10:44:43

Weather

Windvel.	4.90	m/s
Winddir.	79.92	Degs
Humidity	59.26	%
Tempert.	12.00	C-Dg

Radiance

Dir.-1	808.20	W/m2
Dir.-2	788.06	W/m2
Diffuse	51.84	W/m2
Glb.Hrz.	367.08	W/m2
Glb.Gdd.	947.14	W/m2

Circumsolar

Factor	0.00	%

Sun Location

Sol.time	9.69	hrs
Elevat.	21.54	Degs
Azimuth	325.84	Degs
Declin.	-23.11	Degs
Ascens.	259.75	Degs
Longit.	260.58	Degs

Fig.13: Vertical surface temp. profile(measured); in the region of tube 89 at length 3.36m sodium inlet, at 0.635m sodium outlet.

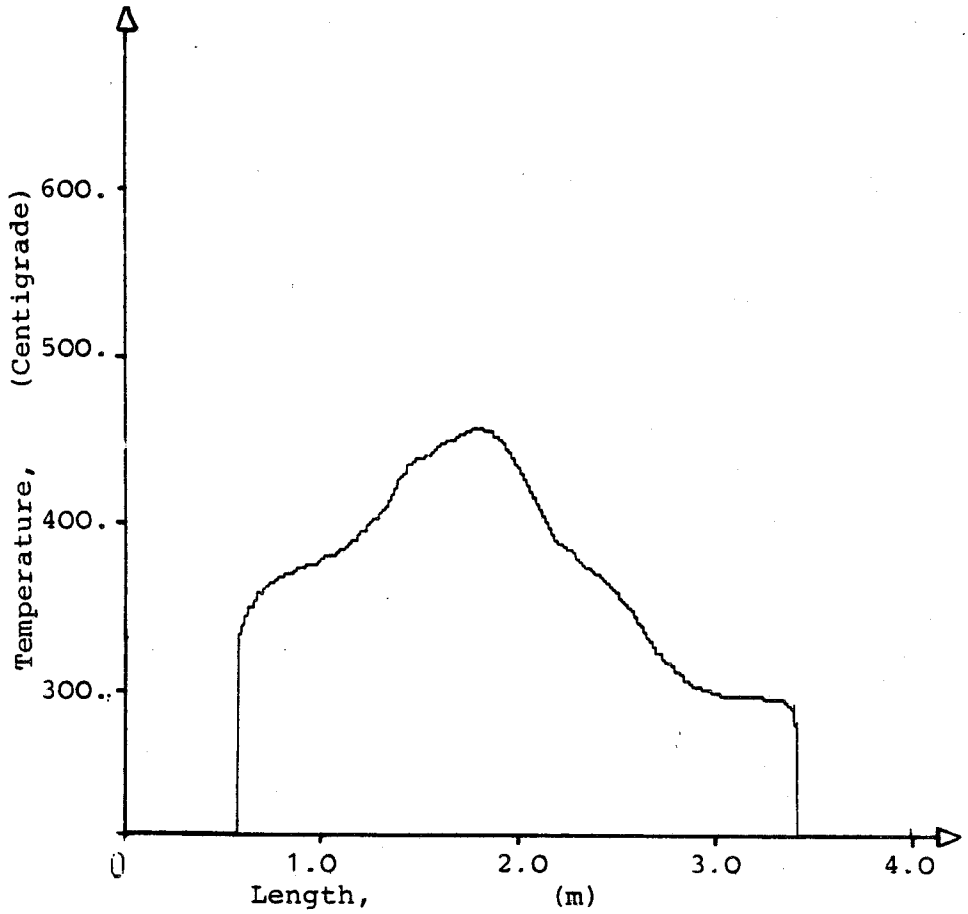

12-Dec-84 10:44:43

Weather

Windvel.	4.90	m/s
Winddir.	79.92	Degs
Humidity	59.26	%
Tempert.	12.00	C-Dg

Radiance

Dir.-1	808.20	W/m2
Dir.-2	788.06	W/m2
Diffuse	51.84	W/m2
Glb.Hrz.	367.08	W/m2
Glb.Gdd.	947.14	W/m2

Circumsolar

Factor	0.00	%

Sun Location

Sol.time	9.69	hrs
Elevat.	21.54	Degs
Azimuth	325.84	Degs
Declin.	-23.11	Degs
Ascens.	259.75	Degs
Longit.	260.58	Degs

Fig.14: Vertical surface temp. profile (measured); near tube 134

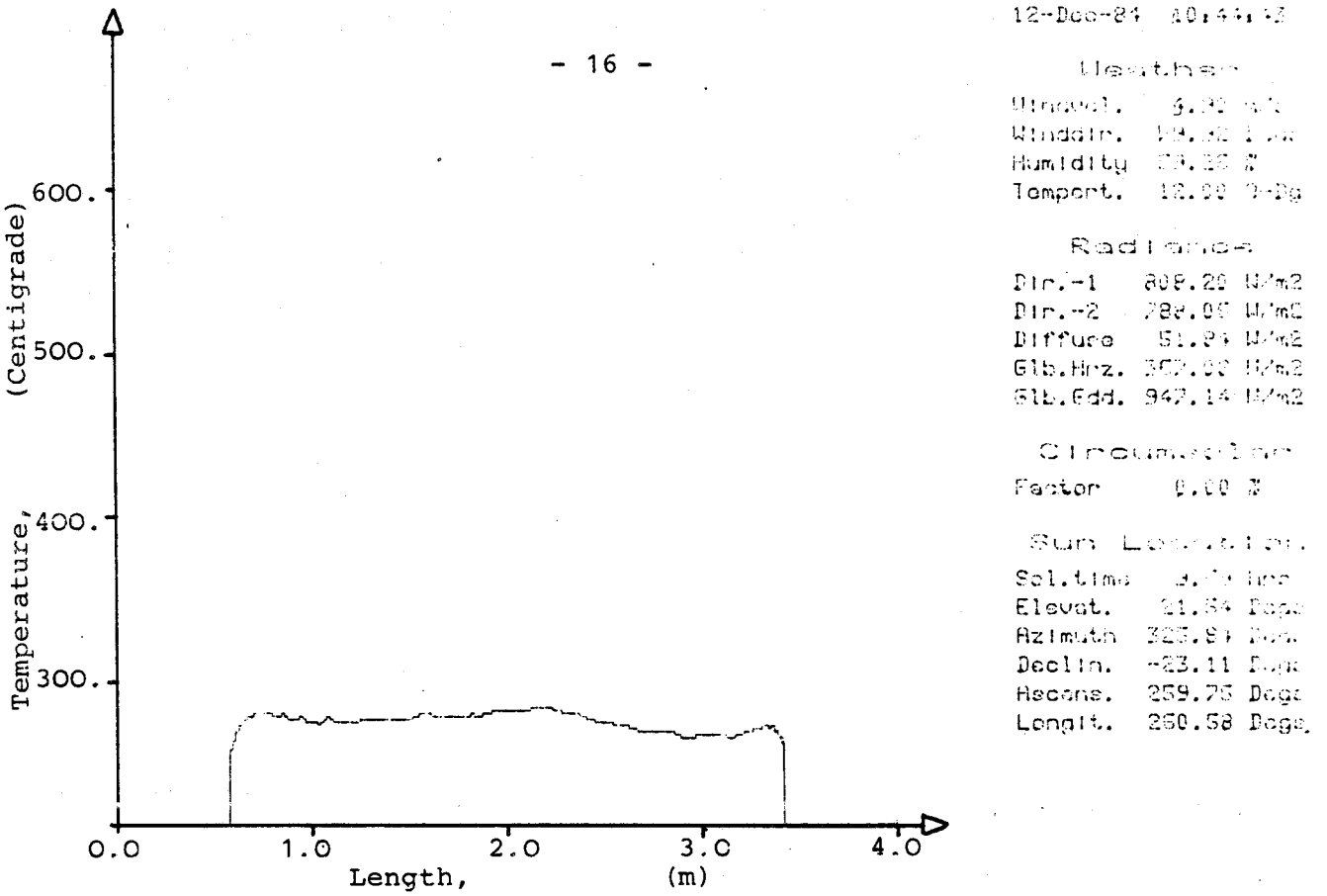

Fig.15: Vertical surface temp. profile (measured), near tube 179; sodium inlet at 3.365m, sodium outlet at .635m.

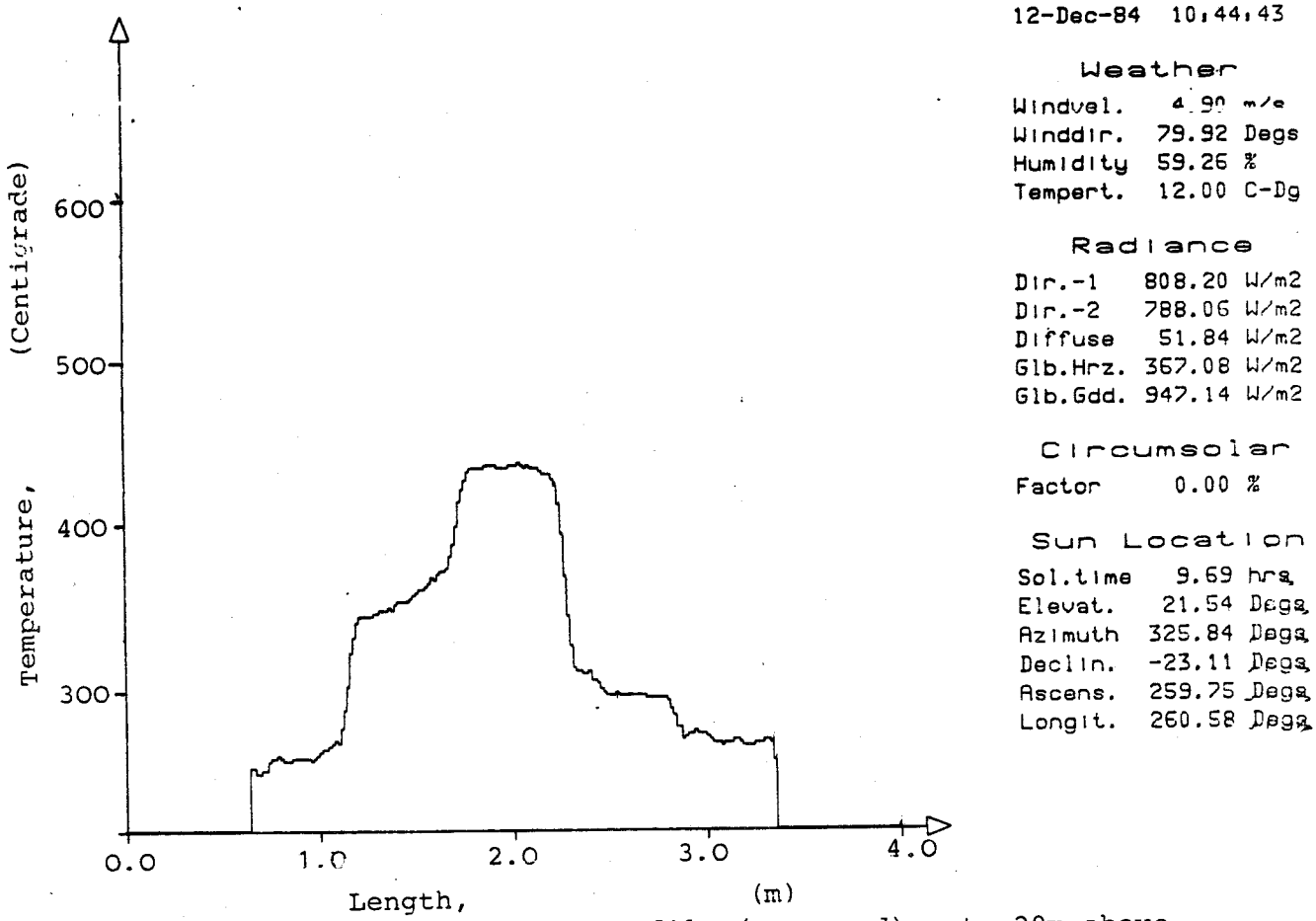

Fig.16: Horizontal surface temp. profile (measured), at .29m above lower aperture rim (panel 1 on left side).

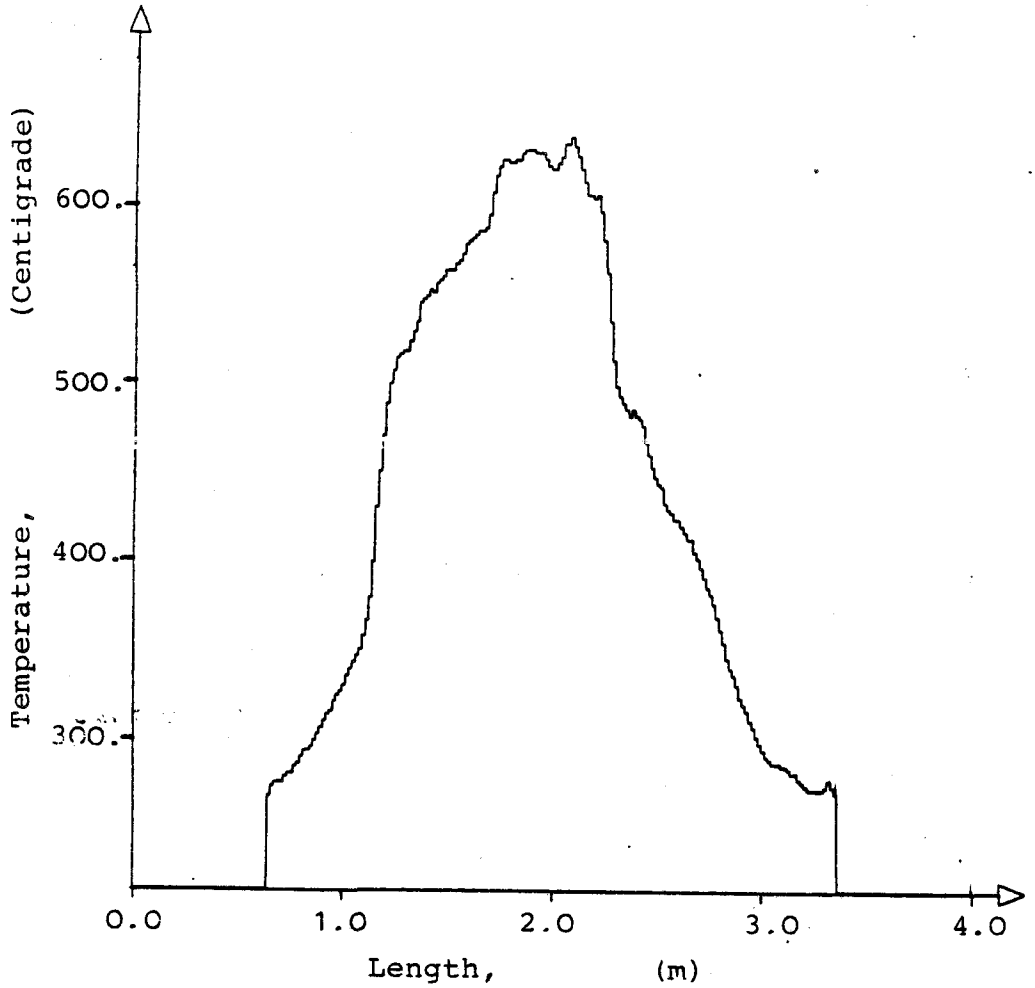

12-Dec-84 10:44:43

Weather

Windvel.	4.90	m/s
Winddir.	79.92	Degs
Humidity	59.26	%
Tempert.	12.00	C-Dg

Radiance

Dir.-1	808.20	W/m2
Dir.-2	788.06	W/m2
Diffuse	51.84	W/m2
Glb.Hrz.	367.08	W/m2
Glb.Gdd.	947.14	W/m2

Circumsolar

Factor	0.00	%

Sun Location

Sol.time	9.69	hrs
Elevat.	21.54	Degs
Azimuth	325.84	Degs
Declin.	-23.11	Degs
Ascens.	259.75	Degs
Longit.	260.58	Degs

Fig.17: Horizontal surface temperature profile (measured by Infrared Camera, HERMES); at 1.86m above lower aperture rim; panel 1 on left side.

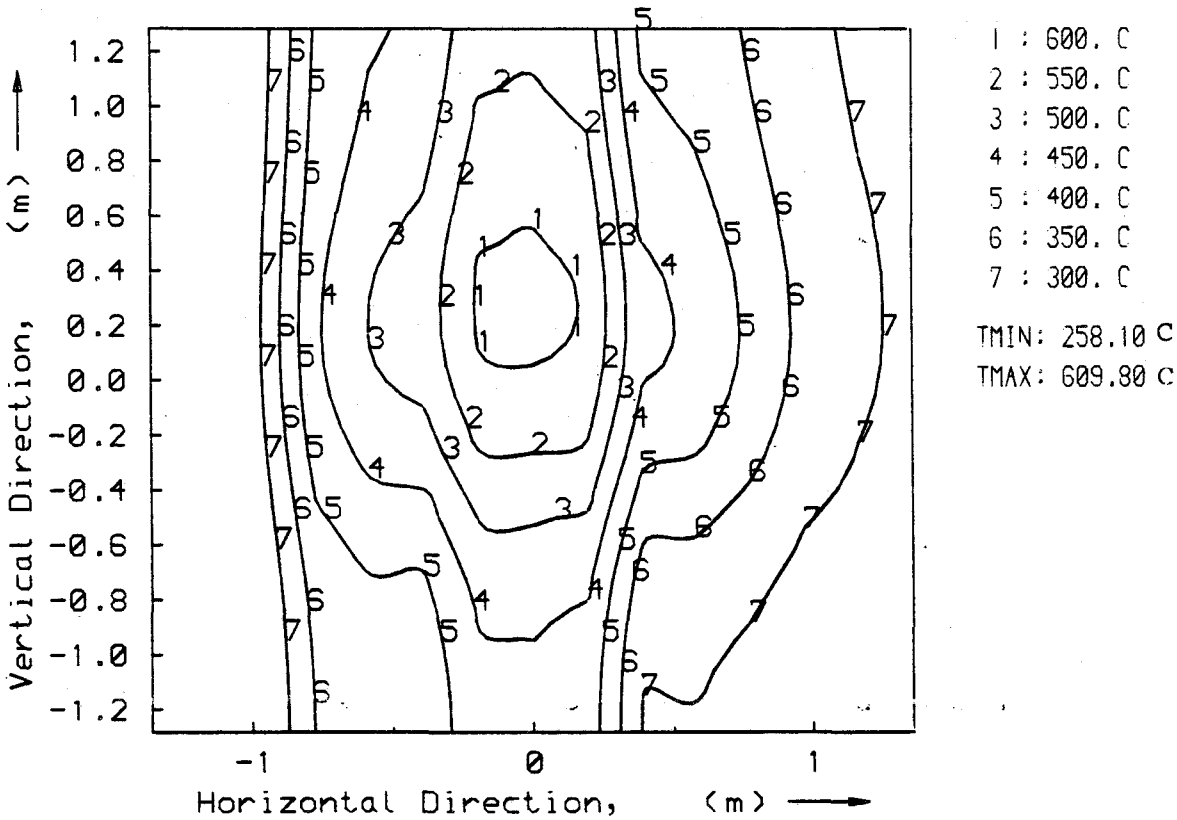

Fig.18: Isothermal lines of front surface ASR (Pyromark coating); calculated by simulation program (HOTREC), has to be compared with Fig.9 ; input datas for steady state on 12-Dec-84 10:44:43.

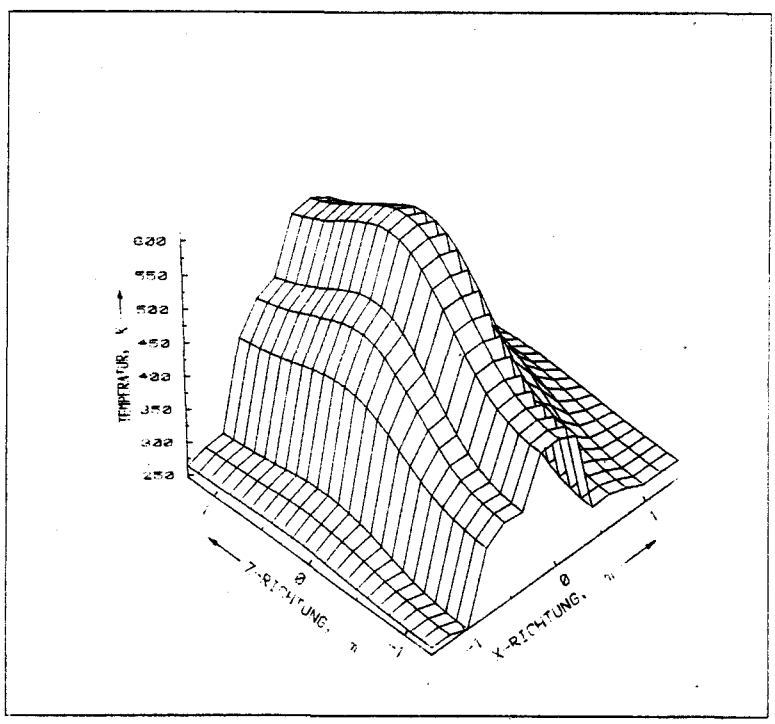

Fig.19: 3D-Presentation of front surface temp. distribution (calculated)

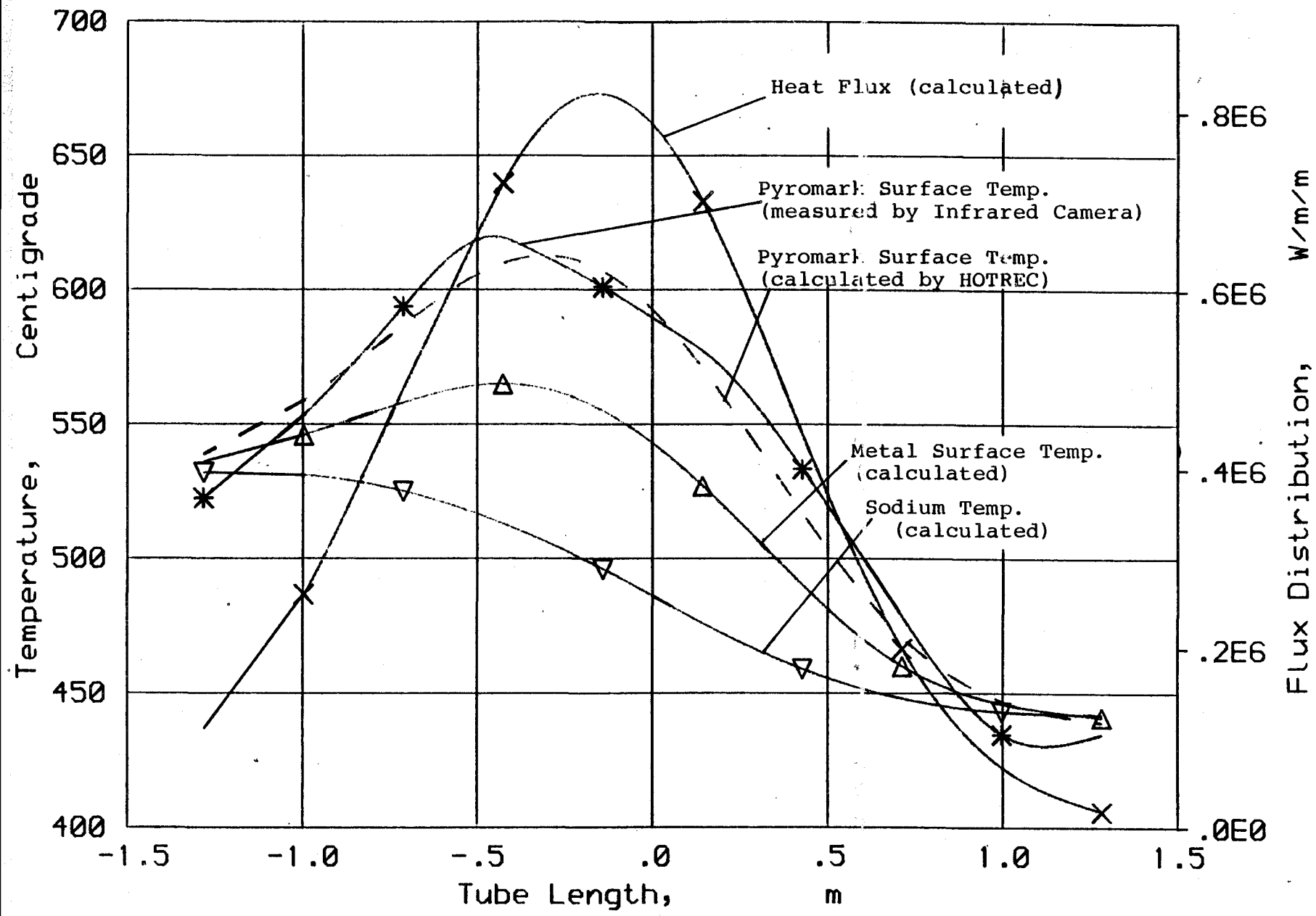

Fig.20: Comparison of calculated and measured temperature profiles for steady state conditions on 12-Dec-84 10:44:43h; temperatures and heat flux profiles of tube 98.

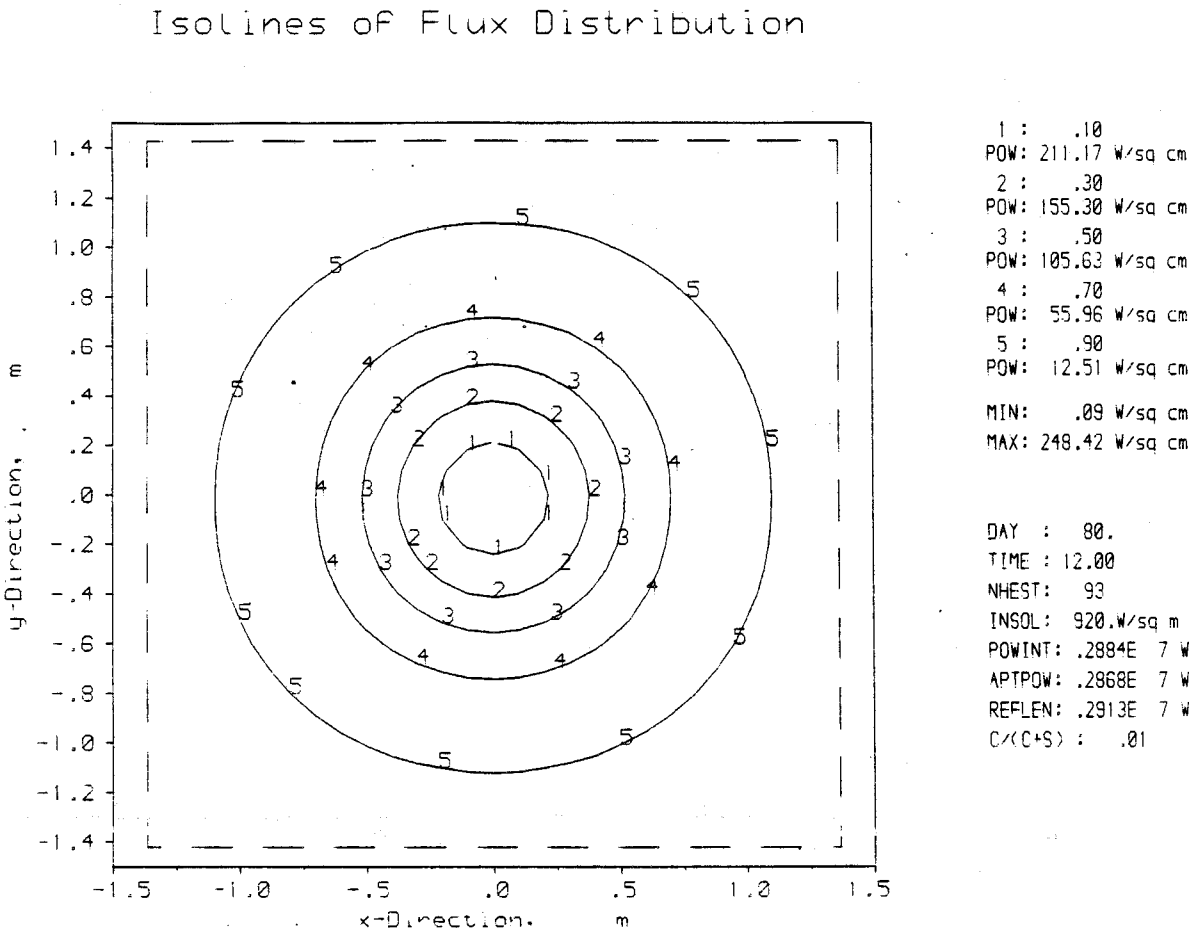

Fig.21: Flux distribution for High Flux Experiment; one aim point (O.,O.) only Martin Marietta heliostats.

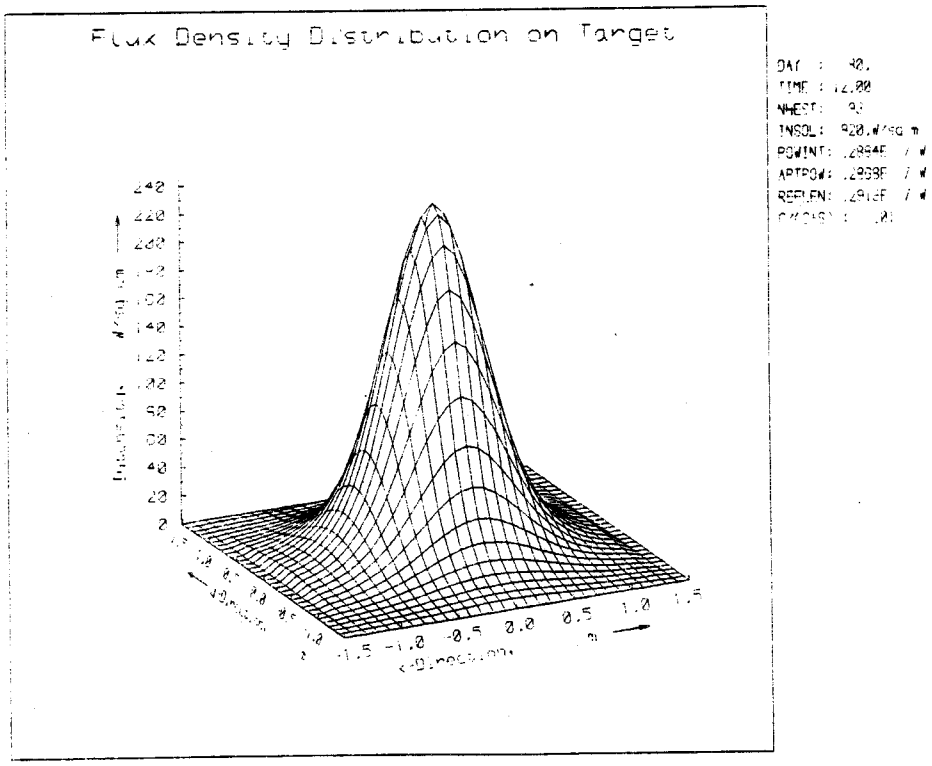

Fig.22: Flux distribution for High Flux Experiment; one aim point.

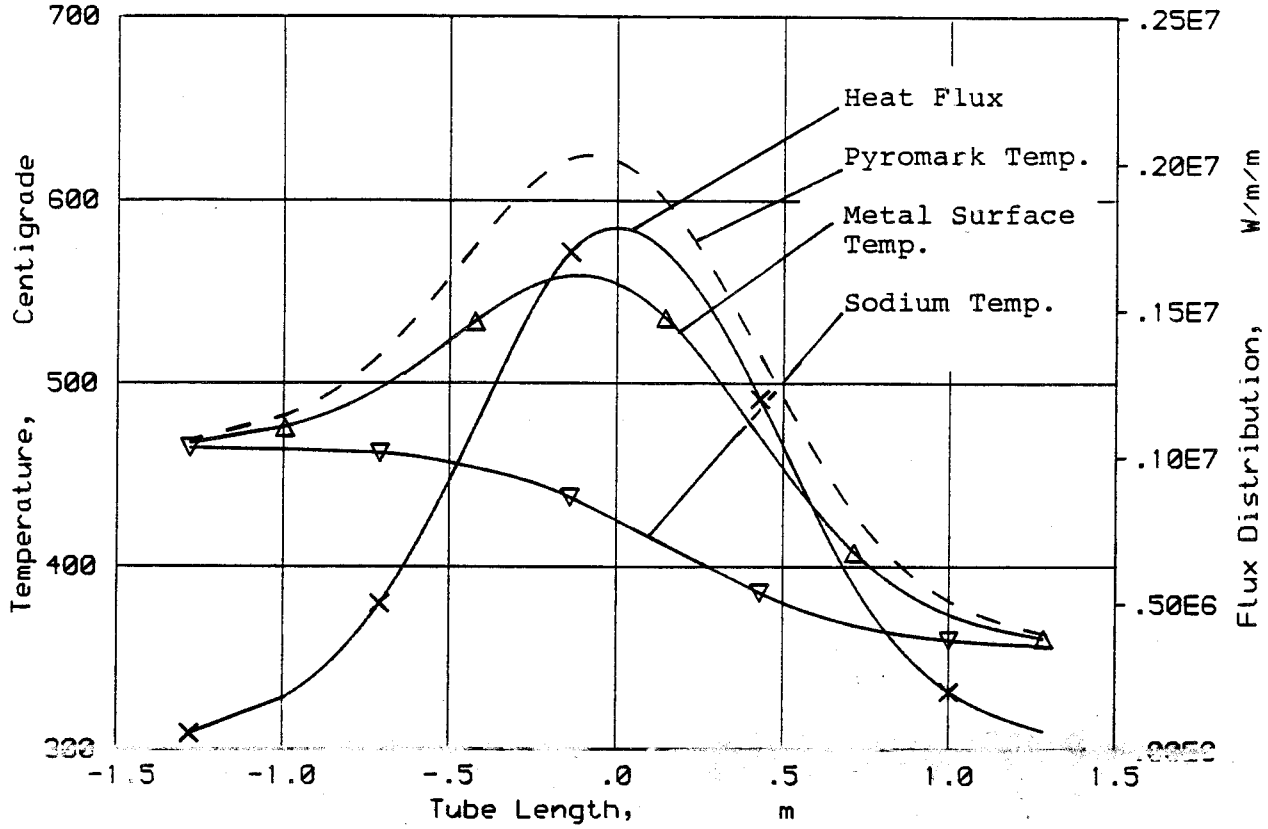

Fig.23: Temperature and heat flux profiles vs. tube length (tube 78) for High Flux Experiment; calculated by HOTREC.

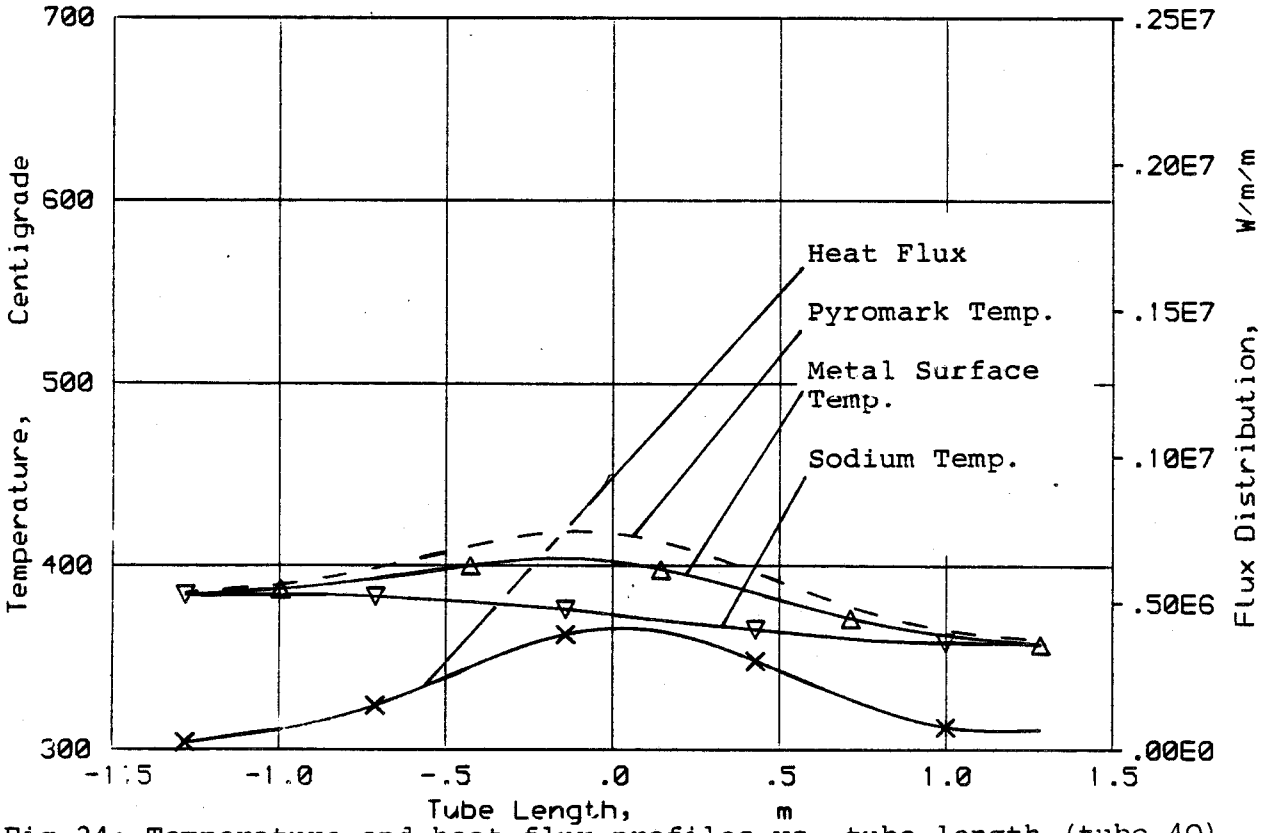

Fig.24: Temperature and heat flux profiles vs. tube length (tube 40) High Flux Experiment

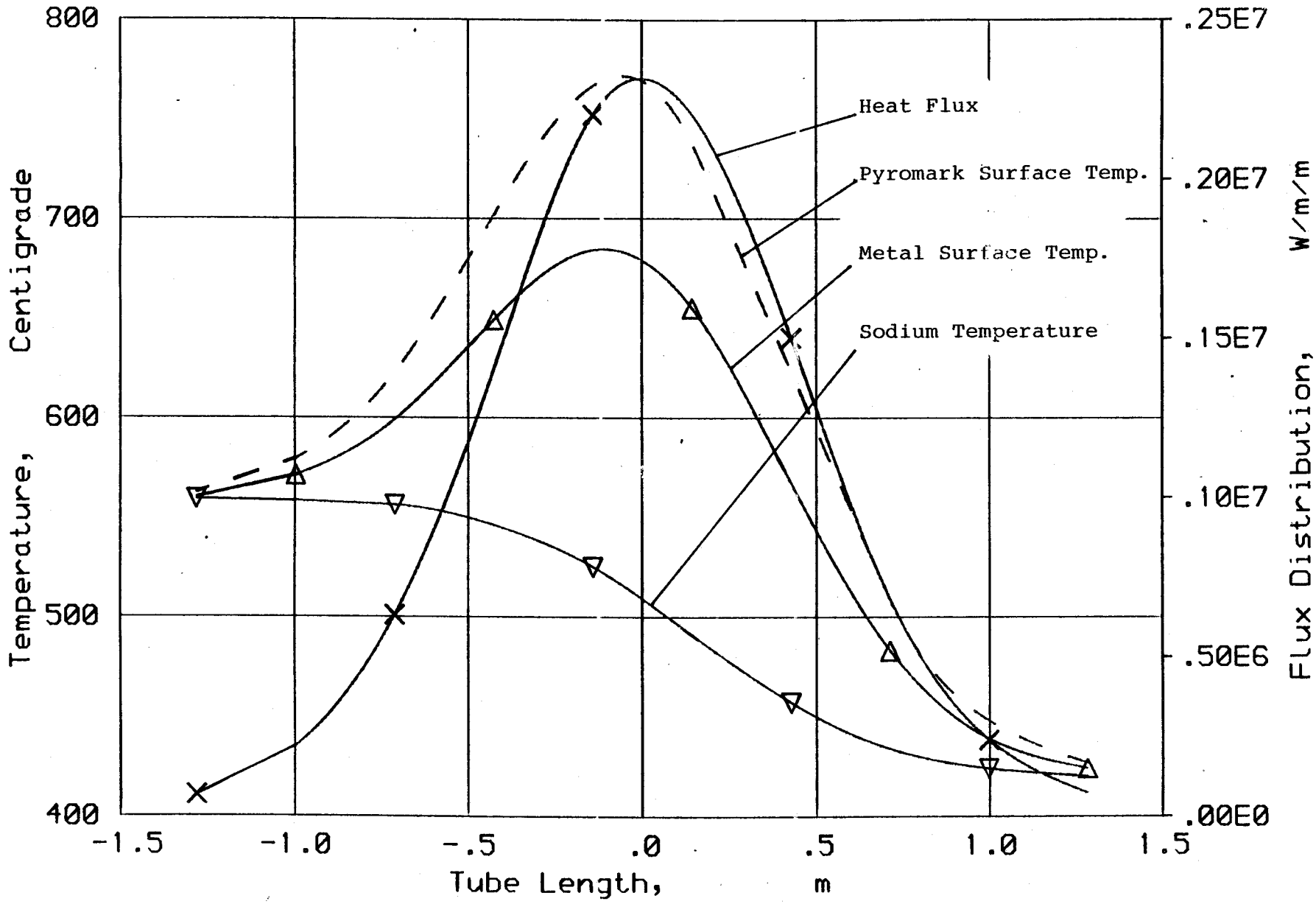

Fig.25: Temperature and heat flux profiles vs. tube length (tube 98) for High Flux Experiment; calculated by HOTREC.

SSPS TECHNICAL REPORTS

1/79	HELIOSTAT FIELD AND DATA ACQUISITION SUBSYSTEM FOR CRS (BY MARTIN MARIETTA)	DECEMBER 1979
2/79	CRS-HELIOSTAT FIELD, INTERFACE CONTROL AND DATA ACQUISITION SYSTEM (BY McDONNEL DOUGLAS)	DECEMBER 1979
1/80	COLLECTOR QUALIFICATION TESTS FOR THE IEA 500 KW_e DISTRIBUTED COLLECTOR SYSTEM (BY SANDIA AND DFVLR)	JULY 1980
2/80	ANALYSIS OF SPECIAL HYDRAULICAL EFFECTS IN THE SHTS PIPING SYSTEM (BY BELGONUCLEAIRE)	NOVEMBER 1980
3/80	REDESIGN OF THE CRS-ALMERIA RECEIVER APERTURE AND COMPARISON OF INTERATOM AND MMC REFERENCE HELIOSTAT FIELD PERFORMANCE CALCULATIONS (BY INTERATOM)	NOVEMBER 1980
1/81	TABERNAS METEO DATA ANALYSIS BASED ON EVALUATED DATA PREPARED BY THE SSPS O.A. (BY BELGONUCLEAIRE)	JUNE 1981
2/81	DCS INSTRUMENTATION REVIEW (BY BELGONUCLEAIRE)	JUNE 1981
3/81	CRS INSTRUMENTATION REVIEW (BY BELGONUCLEAIRE)	JUNE 1981
4/81	INTERNATIONAL ENERGY AGENCY SMALL SOLAR POWER SYSTEMS (SSPS) PROJECT REVIEW (JANUARY 1981) (BY A.F. BAKER, SANDIA)	JULY 1981
5/81	DEVICE FOR THE MEASUREMENT OF HEAT FLUX DISTRIBUTIONS (HFD) NEAR THE RECEIVER APERTURE PLANE OF THE ALMERIA CRS SOLAR POWER STATION (BY DFVLR)	NOVEMBER 1981
6/81	DETERMINATION OF THE SPECTRAL REFLECTIVITY AND THE BIDIRECTIONAL REFLECTANCE CHARACTERISTICS OF SOME WHITE SURFACES (BY DFVLR)	DECEMBER 1981
1/82	SSPS WORKSHOP ON FUNCTIONAL AND PERFORMANCE CHARACTERISTICS OF SOLAR THERMAL PILOT PLANTS PART I, RESULTS OF THE DCS-PLANT SESSIONS (BY A. KALT, DFVLR) PART II, RESULTS OF THE TOWER FACILITIES SESSION (BY M. BECKER, DFVLR)	 APRIL 1982 JULY 1982
2/82	CONCENTRATED SOLAR FLUX MEASUREMENTS AT THE IEA SSPS SOLAR CENTRAL RECEIVER POWER PLANT, TABERNAS - ALMERIA (SPAIN) (BY G. VON TOBEL, CH. SCHELDERS, M. REAL, EIR)	APRIL 1982

SSPS TECHNICAL REPORTS (CONTD.)

3/82	EFFECT OF SUNSHAPE ON FLUX DISTRIBUTION AND INTERCEPT FACTOR OF THE SOLAR TOWER POWER PLANT AT ALMERIA (BY G. LEMPERLE, DFVLR)	SEPTEMBER 1982
1/83	DCS-MIDTERM WORKSHOP PROCEEDINGS (EDITED BY A. KALT, J.G. MARTIN)	FEBRUARY 1983
2/83	FH-PTL WEDEL REFLECTOMETER, TYPE 02-1, NO. 3 FINAL REPORT AND REPORT ON THE TEST PROGRAM (BY G. LENSCH, K. BRUDI, P. LIPPERT, FACHHOCHSCHULE WEDEL)	MARCH 1983
3/83	THE ADVANCED SODIUM RECEIVER (ASR) - TOPIC REPORTS - (BY AGIP NUCLEARE AND FRANCO TOSI)	MAY 1983
4/83	CRS-MIDTERM WORKSHOP (EDITED BY M. BECKER, DFVLR)	JUNE 1983
5/83	INVESTIGATIONS AND FINDINGS CONCERNING THE SODIUM TANK LEAKAGES (EDITED BY W. BUCHER, DFVLR)	JULY 1983
6/83	FIRST YEAR AVERAGE PERFORMANCE OF THE SSPS DCS PLANT (BY TH. VAN STEENBERGHE, SSPS-ITET)	JULY 1983
7/83	THERMAL LOSSES OF THE SODIUM STORAGE VESSELS OF THE CENTRAL RECEIVER SYSTEM. (BY H. JACOBS)	NOVEMBER 1983
1/84	EXECUTIVE SUMMARY - IEA/SSPS - CRS WORKSHOP (APRIL 1983) (BY CLIFFORD S. SELVAGE, SSPS-ITET)	MARCH 1984
2/84	SSPS-DISTRIBUTED COLLECTOR SYSTEM, PROCEEDINGS OF THE INTERNATIONAL WORKSHOP "THE FIRST TERM" (DECEMBER 6-8, 1983, TABERNAS/SPAIN)	MAY 1984
3/84	SESAM-DCS, A COMPUTER CODE FOR SOLAR SYSTEM MODELLING PART I - ANALYSIS REPORT PART II - HOW TO USE (BY J.P. FABRY, H. RICHEL, H. LAMOTTE, M. VEREB, P. BRUSSELAERS)	MARCH 1984
4/84	THE CONTROL OF LARGE COLLECTOR ARRAYS: THE SSPS EXPERIENCE (BY R. CARMONA AND J.G. MARTIN)	JUNE 1984
5/84	SSPS - DCS PLANT PERFORMANCE "THE STAIR-STEP" (BY P. WATTIEZ, J.G. MARTIN, M. ANDERSSON)	JUNE 1984
6/84	AVAILABILITY AND OPERATION FREQUENCY OF SOLAR THERMAL SYSTEMS (BY BELINDA WONG SWANSON)	DECEMBER 1984
7/84	IEA - SSPS CRS CALIBRATION REPORT - CALIBRATION OF RELEVANT MEASURING SENSORS (BY A. BRINNER, DFVLR)	DECEMBER 1984
1/85	PROCEEDINGS OF THE IEA-SSPS EXPERTS MEETING ON "HIGH TEMPERATURE TECHNOLOGY AND APPLICATION", ATLANTA, USA, JUNE 18-21, 1985	JUNE 1985
2/85	ASR - THERMODYNAMICS, RESULTS OF A NUMERICAL SIMULATION AND SURFACE TEMPERATURE MEASUREMENTS	OCTOBER 1985

DISTRIBUTION LIST

1)	SSPS EXECUTIVE COMMITTEE	L. GUTIERREZ (EC CHAIRMAN)	
		G. FANINGER	(A)
		F. ALTDORFER	(B)
		P. KESSELRING	(CH)
		C.-J. WINTER	(D)
		L. CRESPO RODRIGUEZ	(E)
		C. PENCHE SELGUEROSO	(E)
		A. DEL RÍO DISDIER	(E)
		CH. ARONIS	(GR)
		F. REALE	(I)
		B. FINNSTRÖM	(S)
		CH. CARWILE	(USA)
2)	IEA - SECRETARIAT	P.J. HEINZELMANN	
3)	B M F T	G. EISENBEISS	
4)	KFA-PLE	F.J. FRIEDRICH	
5)	ASINEL	J.M. FLUXÁ CEVA J. DE MARCOS PEÑALBA	
6)	SANDIA LABORATORIES	A. BAKER	(3)
7)	D F V L R	(10)	
8)	OPERATING AGENTS	(20)	
9)	SEVILLANA	F. RUÍZ MUÑOZ	(3)
10)	BELGONUCLÉAIRE	G. DEBIER	
11)	INTERATOM	D. STAHL	
12)	M.A.N. - NEUE TECHNOLOGIE	J. FEUSTEL	
13)	MARTIN MARIETTA CORP.	H.C. WROTON	
14)	AGIP SPA	G.C. SCARPI	
15)	FRANCO TOSI	P. CAVALLERI	
16)	SULZER	H. FRICKER	
17)	ACUREX	J. CLARK	
18)	TECNICAS REUNIDAS	P. PEZUELA	
19)	SAIT	H. VANDENBERGHE	